

Material versatility using replica molding for large-scale fabrication of high aspect-ratio, high density arrays of nano-pillars

Y Li¹, H W Ng², B D Gates² and C Menon¹

¹ MENRVA Research Group, School of Engineering Science, Simon Fraser University, 8888 University Drive, Burnaby, BC, V5A 1S6, Canada.

² Department of Chemistry and 4D LABS, Simon Fraser University, 8888 University Drive Burnaby, BC, V5A 1S6, Canada.

E-mail: cmenon@sfu.ca

Abstract

Arrays of high aspect-ratio nano-pillars have attracted a broad interest for various applications, such as for use in solar cells, surface acoustic sensors, tissue engineering, bio-inspired adhesives and anti-reflective surfaces. Each application may require a different structural material, which can vary in the required chemical composition and mechanical properties. In this paper, a low cost fabrication procedure is proposed for large scale, high aspect-ratio and high density arrays of nano-pillars. The proposed method enables the replication of a master with high fidelity, using the subsequent replica molds multiple times, and preparing arrays of nano-pillars in a variety of different materials. As an example applied to bio-inspired dry adhesion, polymeric arrays of nano-pillars are prepared in this work. Thermoset and thermoplastic nano-pillar arrays are examined using an atomic force microscope to assess their adhesion strength and its uniformity. Results indicate the proposed method is robust and can be used to reliably prepare nano-structures with a high aspect-ratio.

1. Introduction

The advancement of innovative fabrication technologies, such as electron beam lithography (EBL) [1-3], nano-imprint lithography (NIL) [4-6], and deep reactive ion etching (DRIE) [7], have enabled the development of a large number of novel nano-structured devices. Arrays of high aspect-ratio (AR) pillars continue to receive widespread interest among many nano-structured devices. Applications include solar cells [8-9], surface acoustic sensors [10-11], structural frames for tissue engineering [12], anti-reflective instruments [13], super-hydrophobic surfaces [14], and bio-inspired dry adhesives [15-17]. While the topographic profile of these nano-structured devices is very similar, their materials are rather diverse. For example, solar cells use semiconducting materials [8-9], and acoustic wave resonance sensors are constructed from metals and piezoelectric materials [10-11], and anti-reflective devices usually utilize

transparent plastics [13]. On the other hand, bio-inspired dry adhesives [15], cell growing beds [18-19], microfluidic devices [20], and super-hydrophobic self-cleaning surfaces [21] are often prepared using a variety of polymers. The development of a novel manufacturing method that could enable the reproduction of the same pattern using a variety of different materials would be desirable. This work aims to widen the choice of materials we are able to replicate using the same soft mold, which would lower the overall cost of fabricating large scale arrays of high AR nano-pillars.

The fabrication of arrays of high AR nano-pillars is generally expensive as it involves the use of sophisticated masks and expensive equipment and instrument setup, which very often have a low throughput. For example, minimum feature size is limited by the wavelength of light used in traditional photolithography processes and, therefore, the use of more sophisticated equipment is required to achieve smaller dimensions [22]. Alternatively, EBL and focused ion beam (FIB) lithography that can create nano-scale features require a relatively long time for direct writing into photoresist or other materials of interest [1-3, 23]. Nano-imprint lithography can greatly reduce the cost of making replicas, but fabricating the silicon masters still requires the use of EBL or FIB processes with a high overall cost to prepare the templates [4-6]. Colloidal masks [24-25] prepared from the self-assembly of polymer beads can facilitate control over both feature size and coverage of large areas, but the precise control over the uniformity in the single layer polymer beads can be a challenge during fabrication. A method that may reduce the time and cost of fabricating arrays of nano-pillars could rely on the use of nano-templates, such as polycarbonate (PC) membranes. However, the pores in PC membranes lack the necessary periodicity to be suitable for creating uniformly distributed nano-pillars [26].

An alternative solution is to use anodic aluminum oxide (AAO) membranes as nano-templates. Membranes of AAO formed by a two-step anodization have been pursued for replication of nano-pillars as they have highly ordered arrays of hexagonal cells, each with a cylindrical pore that can span the entire substrate [27-30]. Pore periodicity, density and diameter—usually down to a hundred nanometers or less—can be finely controlled by the choice of acid and anodization voltage. The fabrication of this type of nano-structure is well established and large sheets of AAO membranes are available by either preparation in the laboratory or from commercial suppliers. The highly uniform membranes of regular nano-sized holes have attracted a large interest as suitable for use as templates to fabricate arrays of pillars [31-43].

Various methods can be used to fill material the array of voids within an AAO nano-template. These methods include atomic layer deposition (ALD), which can grow metal or oxide pillars in the AAO template [31-33]. Another method is electroplating that can deposit various metals in the pores followed by release of the metal nano-wires from the template [34-35]. Chemical vapor deposition (CVD) can grow carbon nanotubes inside the template and can form a uniform nano-forest [36-37]. Hot embossing can be used to fill in the AAO template with thermo-plastic materials [38-44]. Among these methods, hot embossing appears to be an advantageous method to fabricate polymeric pillar arrays. By finely controlling the temperature and pressure of the hot embossing process, Teflon® [39], poly (methyl methacrylate) (PMMA) [40], UV curable polymers [41], polypropylene [42], polyimide [43] and polycarbonate (PC) [44] pillared arrays can be prepared with a range of desired diameters and aspect-ratios for various applications.

In this work, we report a replica molding method based on hot embossing that enables the preparation of arrays of nano-posts from different materials. The use of different materials is a key aspect of this work in order to satisfy the needs of multiple applications [8-21] and also enables the ability to experimentally assess the advantages that specific materials can provide. The method proposed herein shows the feasibility of manufacturing high AR (approximately 25) arrays of nano-pillars (diameter from 200 nm and below) covering large surfaces. One of its specific features is that the proposed method yields high AR nano-pillars that do not collapse, a primary drawback of most manufacturing processes proposed in

the literature [38-44]. Another specific feature is that the process does not require the use of clean-room facilities, which drastically reduces the cost related to the required infrastructure. The proposed process enables the control of both diameter and length of the pillars by opportunely selecting the appropriate nano-template and processing conditions.

2. Sample preparation and evaluation methods

There are mainly three steps for the replication process proposed in this work. First, the thermoplastic pillars are fabricated through a hot embossing process. Second, the polydimethylsiloxane (PDMS) negative replica is cast from the polymeric pillars. Last, other materials, such as thermoset plastics, are cast against the negative PDMS replica containing arrays of holes to prepare the positive replica. By the end of the process, these thermoset plastics have features with the same shape and dimensions as the initial thermoplastic pillars. The overall process is illustrated in Figure 1.

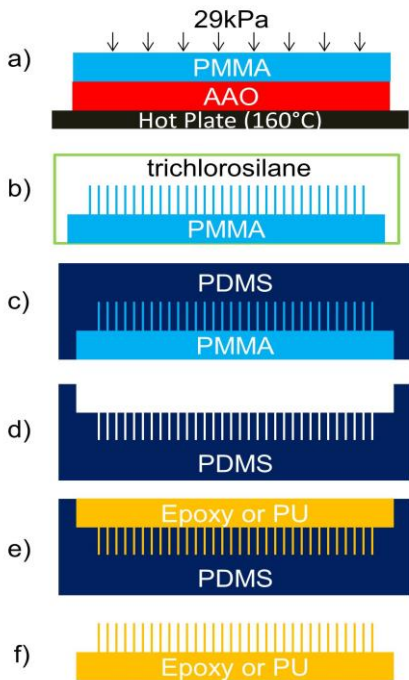


Figure 1. Overall fabrication process to demonstrate material versatility using replica molding of nano-fibrillar arrays: a) thermoplastic PMMA was initially embossed with an anodic aluminum oxide (AAO) template at 160 °C under 29 kPa pressure; b) a silanization procedure created a release layer for the subsequent molding steps; c) PDMS precursors were cast against the PMMA fibrillar structure and cured; d) PDMS negative mold was released from the PMMA master; e) epoxy was cast and thermally cured against the PDMS mold containing an array of holes; f) epoxy replica was released from the PDMS mold, having same shape and dimensions of the arrays of PMMA pillars.

2.1. Fabrication of arrays of nano-pillars in PMMA using AAO

Arrays of thermoplastic pillars were obtained from the AAO template during the first fabrication step, as shown in Figure 1a. Specifically, a commercially available AAO membrane (Whatman© Anopore™ inorganic membrane, Anodisc™ 25) was used in this work. PMMA (OPTIX® acrylic) was selected as the thermoplastic test substrate because of its low glass transition temperature (105 °C), low refractive index

(1.49) and high elastic modulus (3.37 GPa) [45], which reduces the possibility of the pillars collapsing upon release from the mold. A 1 mm thick PMMA sheet was initially cut into 25 x 25 mm² pieces using a CO₂ laser cutter (VLS3.60, Universal Laser Systems) to cover the circular AAO membrane, which had a 21 mm diameter. A hot embossing setup was prepared in the laboratory. The setup included a hot plate (HS40A, Torrey Pines Scientific), two glass slides (Corning® Glass Slides, 75 x 50 mm) used as backing layers to sandwich the AAO template and the PMMA substrate, and a 1 liter volume glass beaker, which was used to provide the necessary embossing pressures.

The following three parameters were fine-tuned to achieve the desired aspect-ratio of the nano-pillars: i) pressure; ii) temperature; and iii) embossing time. The beaker was filled with up to one liter of water to provide ~10 N embossing force. This load was applied over a 346 mm² area, yielding a 29 kPa embossing pressure. The load was applied while the PMMA substrate was heated to just above its melting temperature (148-157 °C [45]). Specifically, it was experimentally determined that 160 °C for the embossing temperature under the 29 kPa load formed a low AR nano-structure in about 15 min. It should be noted that this embossing time does not include the ramp up of the hot plate, which had a maximum ramp rate of 450 °C/hr.

Following the hot embossing process, the samples were cooled without any added pressure until reaching room temperature. Mold release was achieved by etching the AAO template in a NaOH (3 M) solution for ~15 minutes. The samples were subsequently washed with deionized water and dried under a stream of N₂ gas.

This first fabrication step yielded positive PMMA molds having arrays of nano-posts. Different aspect-ratios of the nano-posts were obtained by varying the embossing time, while keeping pressure and temperature at 29 kPa and 160 °C, respectively.

2.2. Fabrication of arrays of nano-holes in PDMS

A negative mold was obtained by casting PDMS (Sylgard 184, Dow Corning) against the arrays of PMMA nano-pillars. To ensure mold integrity after demolding, a release layer was applied to guarantee proper mold release (Figure 1b). A solution phase silanization process was used to deposit this release layer onto the surfaces of the nano-pillars. The PMMA nano-structured sample was placed in an air based plasma (PDC-001, Harrick plasma) at a pressure of ~0.3 Torr for 1 min at 10.7 W to activate the surfaces. The sample was subsequently placed into a flask containing 50 mL hexanes (ACS reagent grade, 98.5%) and 200 µL of silane (1H, 1H, 2H, 2H –perfluorodecyldimethylchlorosilane, Alfa Aesar, >90%) heated to 80 °C in an oil bath for 3 h. The sample was rinsed by immersion in a fresh solution of hexanes and dried under a N₂ gas stream after being retrieved from the solution. Part A and B precursors to the PDMS were mixed in a 10:1 (w/w) ratio, respectively, and poured in a petri dish containing the silanized PMMA sample (Figure 1c). The petri dish was subsequently placed in a vacuum chamber in order to degas the sample for 30 min. After degassing, the sample was left to cure at room temperature for 24 h. After curing, the PDMS was peeled away from the petri dish to obtain the negative mold (Figure 1d). This PDMS mold was used for subsequently casting arrays of nano-pillars from different materials.

2.3. Replication of nano-pillar arrays

In order to demonstrate the proposed process for enabling the fabrication of arrays of nano-pillars in different materials, replicas were prepared using two different polymers: i) polyurethane (V-825, BJB enterprise); and ii) epoxy (TC-1622, BJB enterprise). The polyurethane had a shorter curing time (6-8 min working time before reaching its gel point) than the epoxy (with a 2 h working time). The Young's modulus of the polyurethane and epoxy were 12.3 MPa and 12.6 MPa, respectively. Both polymers were mixed from two initial components and subsequently poured over the negative replica or PDMS mold. The samples were degassed in a vacuum chamber and cured at room temperature (Figure 1e). Replicas of

the cured polymer were subsequently peeled away from the PDMS mold to obtain arrays of nano-pillars (Figure 1f).

2.4. Evaluation of quality of the mold and replica

The geometry of the molds and replicas were examined using a scanning electron microscope (SEM) (Strata DB-235 and Nova NanoSEM 430, FEI). Static water contact angle (WCA) measurements (OCA 15, Dataphysics) were conducted to assess the quality of the various surfaces. In these measurements, the volume of the water droplet was set to 0.5 μL . An average contact angle measurement was obtained from 10 independent measurements for each sample from different locations. To demonstrate their potential for use in applications, polymeric arrays of nano-pillars were tested for their adhesion force using an atomic force microscope (AFM, MFP-3D-SA, Asylum Research). A silicon nitride cantilever (NP-O10, Bruker) without a sharp tip was employed in the adhesion measurements, which have been determined to be suitable for evaluating the adhesion properties of the arrays of nano-pillars [46]. To dissipate the surface static charges during these measurements due to the dielectric properties of the polymers, the edges of the samples were painted with silver paste and connected to a conductive wire that was fixed to the metallic surfaces of the AFM acoustic isolation chamber.

3. Results and Discussion

3.1. Properties of arrays of PMMA nano-pillars

In order to obtain nano-pillars of PMMA with different aspect-ratios, a range of embossing times were selected for the process. Figure 2 shows typical SEM images of the top view of the arrays of nano-pillars obtained using 1 and 2 h of embossing time. The PMMA samples that underwent 1 h of embossing did not exhibit significant collapse of the nano-pillars (Figure 2a), but pillars from samples embossed for 2 h collapsed as they were too tall to withstand lateral adhesion forces exerted by nearby pillars (Figure 2b).

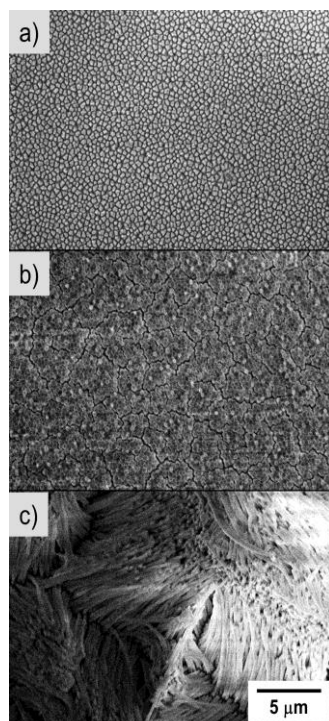


Figure 2. Scanning electron microscopy (SEM) images of the PMMA nano-pillar samples after various embossing times; a) sample prepared by 1 h of embossing; b) sample prepared by 2 h of embossing; c) sample prepared by 1 h of embossing and subsequently treated with Zonyl, which collapsed the pillars and exposed their lengths. All images were obtained at under the same magnification.

The AAO membrane used in the experiments had a thickness of 60 μm , a pore size of 200 nm and pore density of 10^9 pores/ cm^2 [47]. The space between the individual PMMA nano-posts, prepared by the embossing process was very small due to the geometry of the selected AAO membrane. The pores in this template also did not have a very regular pattern or individual shape. The resulting PMMA pillars, therefore, each had a relatively irregular cross-section as shown in Figure 2. It should, however, be noted that the pore size, pore density and the overall membrane size could be further controlled by customizing the anodizing process [27-30]. Nano-posts having different diameters, spacing between pillars, and improved symmetry could potentially be obtained by fabricating a customized AAO membrane.

To estimate the aspect-ratio of the nano-pillars, a cross sectional view of the fabricated PMMA samples is desirable. However, these acrylate samples were difficult to cut through without damaging the nanoscale-features using traditional equipment, such as milling machines, focused ion beams or laser cutters. A fluorinated solvent was used to intentionally collapse the slender pillars and an SEM image obtained to estimate their height (Figure 2c). From the top view of the bent pillars, the average length was estimated to be 5 μm for samples that underwent 1 h embossing time. The aspect-ratio of this sample was estimated to be 25, which greatly exceeds the requirements of most applications mentioned previously.

In the experiments to obtain nano-pillars in different aspect ratios, we chose to vary embossing time while fixing the embossing pressure and temperature. Other approaches to prepare the arrays of nano-pillars could vary the pressure with a fixed embossing time and temperature, or vary temperature with a fixed embossing time and pressure. Any of these methods could be used to calibrate a fabrication process to accurately prepare nano-pillars of specific aspect ratios, once a best method is established to overcome the intrinsic difficulties of systematically and accurately determining the aspect ratio of the nano-pillars.

Figure 3a shows an optical image of the sample containing PMMA nano-pillars, which were obtained from a one hour embossing time. This nano-structured PMMA sample preserved most of the transparency of the original PMMA material because the array of nano-pillars remained upright without collapsing upon release from the AAO mold. The outline of a circular shape in Figure 3a indicates the boundary of the deformed PMMA surfaces that were in contact with the 21 mm diameter polypropylene ring that protected the rim of the brittle AAO commercial membrane. On the other hand, the PMMA samples that underwent a two hour embossing process appeared to have a foggy gray coloration (Figure 3b). This color change was due to the formation of collapsed posts that reduced transparency of the sample.

Figure 3 also shows that the entire embossed area was roughly the size of a C\$ 0.25 coin. This large nano-patterned area was prepared using a single embossing stamp, indicating that the proposed process, which required very affordable fabrication equipment, could potentially provide a high yield manufacturing process.

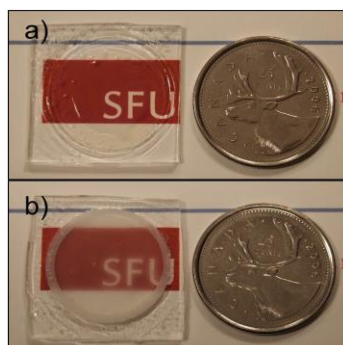


Figure 3. Samples of PMMA nano-pillars placed on top of the SFU logo with a C\$ 0.25 coin placed next to the sample to indicate the scale: a) sample prepared by 1 h of embossing; b) sample prepared by 2 h of embossing.

3.2. Release layer and mold release

A soft polymer was selected to obtain a negative mold from the PMMA positive mold in order to retain the integrity of the PMMA template after demolding. PDMS was chosen for its low viscosity and low surface energy, which facilitated the mold filling and mold releasing processes. However, directly casting PDMS and peeling it away from the very high aspect-ratio PMMA nano-structures could have damaged the PDMS sample due to the low tear strength of PDMS. A release layer of perfluoroalkylsilane molecules was applied to the PMMA samples prior to casting PDMS. Specifically, a solution phase silane deposition process was used to ensure the molecules could reach deep into the trenches of the high AR nano-pillars. Unlike traditional release layers, such as polyvinyl alcohol (PVA) or silicon oil, that are usually applied using spin coating, the perfluoroalkylsilane molecules can coat the surfaces of the nano-pillars using either a gas or solution based medium. These molecules form a thin layer that protects and alters the surface energy of the original mold during the demolding process. Solution based coating processes enable faster and more uniform transport of the silane molecule through the help of a solution media. PMMA is sensitive to a large variety of solvents, leaving few choices for the deposition media. Among this remaining list, hexanes were selected for dispersion of the perfluoroalkylsilane molecules during the deposition process. WCA measurements were performed on the samples nano-pillars after coating with the silane molecules to determine the quality of these coatings. Results and discussion of these WCA measurements are provided in further detailed in the supporting material.

Figure 4a shows SEM images of arrays containing PMMA nano-pillars after demolding of PDMS when the PMMA mold was not treated with the perfluoroalkylsilane release layer. Although PDMS is a material that is widely used in replica molding, we could only release a thin layer of PDMS from the PMMA pillars. The resulting PDMS negative replica had either no nano-holes or holes with a very low aspect-ratio, which were not suitable for subsequent replica molding processes. Figure 4b shows the PMMA sample after demolding of the PDMS when the PMMA was treated with a silane release layer before casting the PDMS. The aspect-ratio of the features in the resulting PDMS negative mold significantly increased following this treatment and facilitated the further use of the PDMS negative mold in subsequent molding steps of the process. However, this PDMS release layer was not perfect, as parts of the PDMS remained trapped deep within the trenches surrounding the PMMA nano-pillars. This phenomenon could be caused either by the very low tear strength of PDMS or by an incomplete coating with silane molecules, which may not cover all surfaces of the nano-pillars. Improvement of the silane treatment process would need to be addressed to enable further improvements in the quality of this replica molding method. An alternative method of silane deposition could be through the use of an atomic layer deposition process, but the appropriate equipment is necessary to perform these studies. Despite the

presence of some defects, the PDMS samples were suitable for use as negative molds and enabled the preparation of arrays of high AR nano-pillars, as discussed in the following sections.

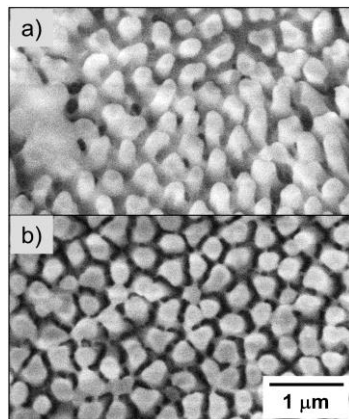


Figure 4. SEM images of dense arrays of PMMA pillars after demolding of PDMS; a) arrays of PMMA pillars that did not utilize a release layer applied prior to casting PDMS; b) arrays of PMMA pillars with a release layer applied prior casting the PDMS. The two SEM images were taken at the same magnification.

3.3. Positive replica using epoxy and polyurethane

Thermoset materials can be cast directly against the AAO template to form nano-pillars. This approach has been reported to have multiple drawbacks including a very limited control over length of the pillars and a subsequent collapse of these fibers [48]. In addition, obtaining the final nano-pillar arrays directly from the AAO membranes would require using one AAO template per casting, which makes the process very expensive for the fabrication of large quantities of nano-pillar containing arrays.

The use of replica molding was, therefore, selected to minimize the use of AAO membranes. Thermoset materials were cast against the PDMS negative molds to obtain the final arrays of nano-posts. Epoxy and polyurethane were both evaluated to prove the proposed method could be used to prepare nano-posts in substantially different materials.

Figure 5 shows SEM images of the fabricated epoxy (Figure 5b) and polyurethane (Figure 5c) nanostructures against the original arrays of PMMA nano-pillars (Figure 5a). It can be seen that the density of pillars decreased for both replicas. Aspect-ratio of both the epoxy and polyurethane based nano-pillars was about 5. The decrease of pillar density and aspect-ratio was primarily attributed to the well-known low wettability of PDMS [49]. The use of vacuum to improve the ability of epoxy or polyurethane to fill the PDMS nano-holes was unsuccessful, possibly due to nano-bubbles of trapped air residing in a large number of the nano-holes. The longer curing time of epoxy (24 h) with respect to polyurethane (~7 min to reach a very viscous phase) negligibly improved the density of the nano-pillars.

Figure 5 also shows that the cross-sectional circumference of the thermoset pillars increased in comparison to the initial PMMA nano-pillars. This phenomenon was attributed to expansion of the nano-pillars during the elastomers' cross-linking phase, which was only partially constrained by the surrounding soft PDMS mold.

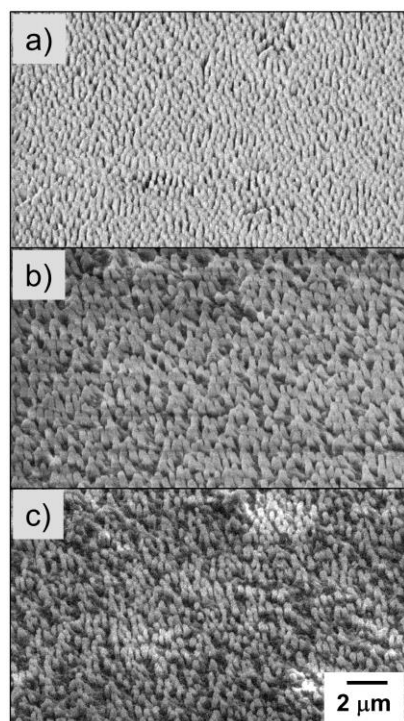


Figure 5. SEM images of the original dense arrays of PMMA nano-pillars (a), epoxy replica of these arrays (b) and a polyurethane replica of the arrays of nano-pillars (c). All of the images were taken at the same magnification and a 45° tilt.

Despite these limitations, arrays of nano-pillars with an AR of 5 were reliably and repeatedly prepared from the same PDMS molds. It should be noted that an aspect-ratio of 5 is suitable for a large variety of applications [9-11, 13-17]. This final step of the process shows that the use of expensive AAO membranes can be limited to the initial fabrication of the PMMA positive molds, but can enable the preparation of a number of replicas from different materials.

3.4. Case study: a bio-inspired dry adhesive

As an example of a potential application, epoxy based arrays of nano-pillars were studied to assess their use as gecko-inspired dry adhesives. These nano-pillars of epoxy were compared to PMMA nano-pillars from the initial positive mold to demonstrate that an appropriate selection of material can increase the adhesion performance of these arrays.

A nanoscopically flat silicon nitride AFM cantilever was controlled to vertically approach the arrays of nano-pillars and stop after reaching a predetermined force. The AFM cantilever was subsequently vertically withdrawn until the fibers detached from the cantilever. This specific motion of the AFM cantilever has been proven to be particularly suitable for evaluating nano-structured gecko-inspired adhesives [46]. The adhesion force between the nano-pillar and the cantilever surface was calculated through deflection of the cantilever. The contact area between the cantilever and the nano-fibrils was estimated to be $\sim 16 \mu\text{m}^2$. In order to gather detailed information on the uniformity of the adhesion force for these surfaces, a program was written to automatically move the cantilever and repeat the aforementioned movements to acquire a large set of measurements over an array, as well as from different locations within the sample. Each unique position was separated by at least $1 \mu\text{m}$. The adhesion forces were plotted in grey scale with a lateral offset of the data corresponding to the physical location where the

measurements were performed on the sample in order to create a force map (Figure 6). The uniformity or variations in the adhesion forces across the sample can be easily visualized by examining the grey scale force maps obtained from different areas. Random patterns and trends in the measured adhesion forces within one force map indicate the anticipated variation for these measurements. The random variation in adhesion forces measured across a sample is the result of randomized test conditions, including a random numbers of pillars interacting with the AFM cantilever during each measurement and small variations in the aspect ratio of those pillars. On the other hand, a localized decrease in adhesion forces within the map indicates the possible presence of defects (e.g., missing fibers). Identification of these defects can help improve the fabrication process. By observing the trends in the appearance of the arrays of nano-pillars and the corresponding force map, the effect of variations in shape, size and density of these nano-pillars can be correlated to the resultant adhesion forces. This method also permits an automated collection of large sets of data, which enable a detailed statistical analysis of adhesion forces for samples in order to characterize their performance as a dry adhesive and the quality of the developed manufacturing process [46].

Figure 6b shows the force map obtained from an array of PMMA nano-pillars, which was prepared by 1 h of hot embossing. An SEM image of the PMMA sample having the same magnification ($20 \times 20 \mu\text{m}^2$) used to obtain the force map is provided in Figure 6a to facilitate the visualization of the area analyzed by the force map within the PMMA sample. It should be noted that the AFM and SEM images do not correspond to an identical region; these images were obtained from two unique regions of the sample, but with the same lateral dimensions. Subsequently testing the adhesion force of a region after imaging with an SEM was avoided as the focused electron beam modifies the surfaces and the geometrical features of the polymer.

The results plotted in Figure 6b indicate that the values of the measured force were random across the tested area without an apparent spatial trend. These results suggest there are small variations across the sample, but this trend in adhesion forces conforms to the variation anticipated for an array of nano-pillars as described above. The adhesion force measurements for the epoxy sample had a larger variation in measured values and in the force maps. For example, the region highlighted with the red oval in Figure 6d shows an area in which adhesion was low, presumably due to the presence of defects in the sample. These defects could be missing or collapsed pillars that reduced the contact area between the epoxy nano-pillars and the AFM cantilever resulting in a decrease in the measured adhesion forces. The PMMA nano-pillars had a better preservation of the original template geometry than the epoxy nano-pillars. The PMMA based pillars could be preferred for a range of optical and biological applications, while the epoxy nano-pillars could be more suitable for use as a dry adhesive.

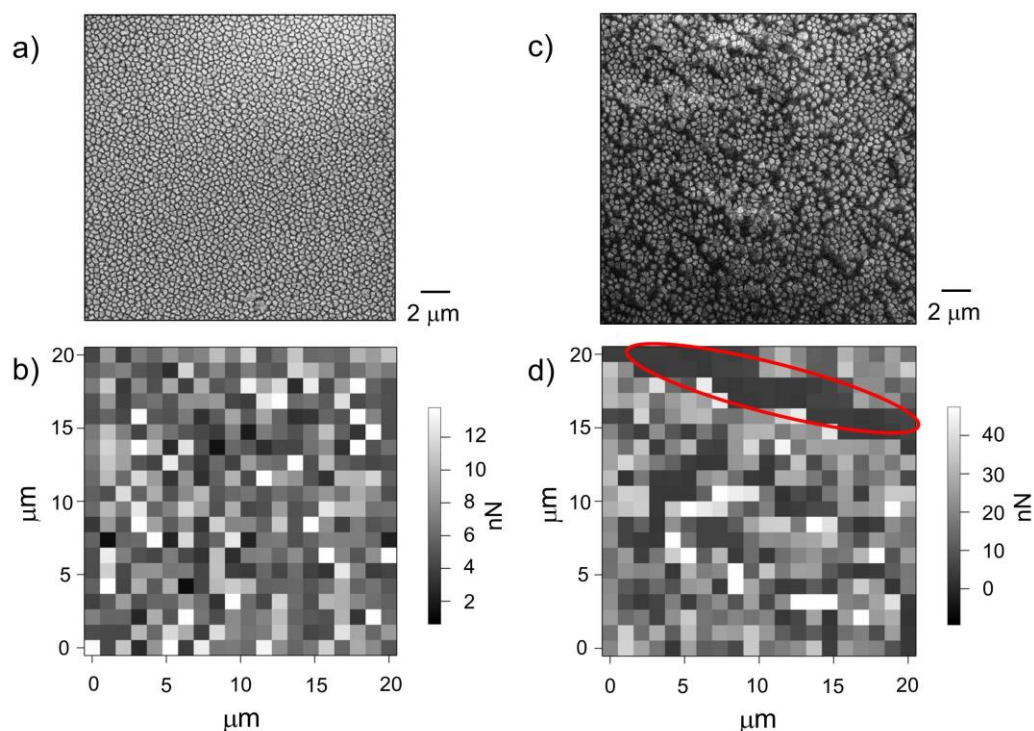


Figure 6. (a) Representative SEM image of a sample containing an array of PMMA pillars whose adhesion forces were measured using an atomic force microscopy (AFM) based technique, and (b) the corresponding force map obtained from these measurements. Both the SEM and force map have the same lateral dimensions. (c) SEM image obtained from a representative region of an array of epoxy pillars whose adhesion forces were measured by an AFM based technique, and (d) a corresponding force map with the same lateral dimensions. All images correspond to an area of $20 \times 20 \mu\text{m}^2$. The red oval in (d) indicates a defect in the sample, possibly due to the partial collapse of neighboring nano-pillars or missing nano-pillars.

Figure 7 shows histograms that summarized the force measurements acquired from the arrays of PMMA and epoxy nano-pillars. In addition, a third histogram was added for a PMMA sample that contains shorter pillars (0.5 h of hot embossing). All of the histograms were obtained by collecting force measurements from a large number of locations (400 points) in order to perform proper statistical analysis. The two histograms for the hot embossed PMMA contain a single peak while analysis of the epoxy replica contains multiple peaks spanning a much larger range of forces. The reason for this discrepancy is that the arrays of PMMA nano-pillars had a more uniform topography than that observed in the epoxy based samples (e.g., compare Figures 6a and 6c). The latter sample had a higher number of defects, such as missing pillars.

For the arrays of PMMA pillars, samples having shorter pillars (prepared using 0.5 h of embossing) induced a lower adhesion force than the taller pillars (from a 1 h embossing process). This difference is shown in both the mean and median of the histograms in Figure 7. The taller pillars may be able to provide a higher flexibility and ability to bend when the AFM cantilever was pressed against these structures. Bending of the pillars might have created an increased contact area between the sides of the pillars and the flat AFM cantilever. These interactions between the nano-structures and the AFM cantilever would correspond to a higher measured adhesive force. While statistically significant, the effect of the AR was not very noticeable; the variation in mean and median for the two PMMA samples was 7.2% and 11.7%, respectively. A much larger variation in the adhesion force was observed within the

epoxy based samples. In fact, despite the decrease in pillar density and aspect-ratio, the measured adhesion for the epoxy samples was more than 3 times higher than that for the PMMA samples. This change was attributed to the higher surface energy of epoxy (44.5 mJ/m^2) with respect to PMMA (37.5 mJ/m^2) [50]. This increase of adhesion supports our conclusion that this method of replicating nano-pillars can be successfully utilized to select the most suitable material for a specific application, in this case the preparation of a biomimetic dry adhesive. It can be envisioned that future research on the preparation of complex structures will take advantage of this replica molding method.

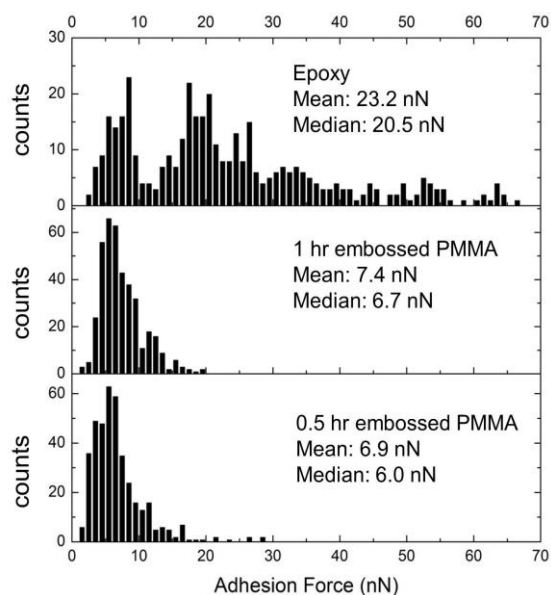


Figure 7. Histograms of the adhesion force measured for samples containing arrays of nano-pillars prepared from epoxy, as well as PMMA nano-pillars prepared using either 0.5 h or 1 h of hot embossing as indicated on these plots. These measurements were obtained using an atomic force microscope, a flat cantilever, and a set of customized software routines for manipulating the cantilever.

The combined analysis of the adhesion maps and histograms (Figures 6 and 7) indicated the presence of defects in the epoxy based samples and a consequent large variation in measured adhesion. It should, however, be noted that the presence of such localized defects is believed to not largely affect the macroscopic performance of the sample because the area occupied by these defects is very small in comparison to the overall surface area of the sample. In addition, a suitable preloading force applied to the sample can potentially create an improved contact with the shorter nano-pillars and, thus, improve the overall adhesion strength of the sample. Despite any possible influence of these defects, an investigation was performed to identify their potential sources. These sources included: 1) PDMS not properly demolding from the PMMA nano-pillars, resulting in a reduced AR and density of the nano-holes in the PDMS mold; 2) the epoxy might not have completely filled the PDMS nano-holes due to its low surface energy; and 3) the epoxy could not properly demold from the PDMS mold (epoxy nano-pillars could remain trapped in the PDMS nano-holes). Figures 2, 5, 6 and 7 each provide evidence that the replication process yielded an array of high quality nano-pillars with high adhesion properties, but future work will tackle the above-mentioned potential causes for defects in the replicated structures to improve the uniformity of the final arrays of nano-pillars.

4. Conclusions

This paper introduces a replica molding technique that enables the preparation of dense arrays of nano-pillars in a variety of materials. This high yield method requires low cost fabrication facilities. A thermoplastic material (PMMA) was pressed against an AAO template to form arrays of high aspect-ratio nano-pillars. The transparency of the nano-structured polymer indicated these nano-pillars retained their upright or columnar structure and did not collapse. The arrays of PMMA nano-pillars were subsequently used as a positive mold to form a PDMS negative mold. A silane based release layer was applied on the PMMA surfaces to enable improved release of this PDMS mold. The quality of the release layer was examined using water contact angle measurements and SEM imaging. Two thermoset plastics, PU and epoxy, were subsequently cast against the PDMS negative molds to obtain positive replicas. The pillar density and shape within these replicas were examined by SEM analysis. As a case study, the adhesion properties of the replicas were investigated for samples containing arrays of nano-pillars that were similar in size and shape to a gecko's setae. The adhesion force for arrays of epoxy (replica) and PMMA (master) nano-pillars were measured using AFM based techniques. The average adhesion force of the epoxy sample was more than three times higher than that of the PMMA sample. This improvement was associated to the higher surface energy of the epoxy. This case study demonstrated that the selection of the structural material could play an important role in the performance of the fabricated nanostructures. The proposed method has an advantage over existing fabrication processes as it enables the selection of a variety of materials from which to fabricate arrays of nanostructures.

Acknowledgements

This work was supported by the Natural Sciences and Engineering Research Council (NSERC) of Canada and the Canada Research Chairs Program (B.D. Gates). This research also made use of 4D LABS shared facilities supported by the Canada Foundation for Innovation (CFI), British Columbia Knowledge Development Fund (BCKDF), Western Economic Diversification Canada, and Simon Fraser University.

References

- [1] Vieu C, Carcenac F, Pépin A, Chen Y, Mejias M, Lebib A, Manin-Ferlazzo L, Couraud L, Launois H 2000 Electronbeam lithography: resolution limits and applications. *Appl. Surf. Sci.* **164** 111-117.
- [2] Grigorescu AE and Hagen CW 2009 Resists for sub-20-nm electron beam lithography with a focus on HSQ: state of the art. *Nanotechnology* **20** 292001.
- [3] Kolodziej CM, Kim SH, Broyer RM, Saxer SS, Decker CG, Maynard HD 2012 Combination of Integrin-Binding Peptide and Growth Factor Promotes Cell Adhesion on Electron-Beam-Fabricated Patterns. *J. Am. Chem. Soc.* **134** 247-255.
- [4] Guo LJ 2007 Nanoimprint lithography: methods and material requirements. *Adv. Mater.* **19** 495-513.
- [5] Lee S-W, Lee K-S, Ahn J, Lee J-J, Kim M-G, Shin Y-B 2011 Highly Sensitive Biosensing Using Arrays of Plasmonic Au Nanodisks Realized by Nanoimprint Lithography. *ACS Nano* **5** 897-904.
- [6] Balla T, Spearing SM, Monk A 2008 An assessment of the process capabilities of nanoimprint lithography. *J. Phys. D: Appl. Phys.* **41** 174001.

- [7] Chekurov N, Grigoras K, Peltonen A, Franssila S, Tittonen I 2009 The fabrication of silicon nanostructures by local gallium implantation and cryogenic deep reactive ion etching. *Nanotechnology* **20** 065307.
- [8] Maiolo III JR, Kayes BM, Filler MA, Putnam MC, Kelzenberg MD, Atwater HA, Lewis NS 2007 High Aspect Ratio Silicon Wire Array Photoelectrochemical Cells *J. Am. Chem. Soc.* **129** 12346-12347.
- [9] Nakayama K, Tanabe K, Atwater HA 2008 Plasmonic nanoparticle enhanced light absorption in GaAs solar cells. *Appl. Phys. Lett.* **93** 121904.
- [10] Ramakrishnan N, Nemade HB 2011 Loading in Coupled Resonators Consisting of SU-8 Micropillars Fabricated Over SAW Devices. *IEEE Sens. J.* **11** 430-431.
- [11] Xua J, Dapinoa MJ, Gallego-Perezb D, Hansfordb D 2009 Microphone based on Polyvinylidene Fluoride (PVDF) micro-pillars and patterned electrodes. *Sensor Actuat. A-Phys.* **153** 24-32.
- [12] Chandra D, Taylor JA, Yang S 2008 Replica molding of high-aspect-ratio (sub-)micron hydrogel pillar arrays and their stability in air and solvents. *Soft Matter* **4** 979-984.
- [13] Shin HG, Kwon JT, Seo YH, Kim BH 2008 Fabrication of Polymer Master for Antireflective Surface Using Hot Embossing and AAO Process. *Int. J. Mod Phys. B* **22** 5887-5894.
- [14] Krishnamoorthy S, Gerbig Y, Hibert C, Pugin R, Hinderling C, Brugger J, Heinzelmann H 2008 Tunable, high aspect ratio pillars on diverse substrates using copolymer micelle lithography: an interesting platform for applications. *Nanotechnology*, **19** 285301.
- [15] Choi MK, Yoon H, Lee K, Shin K 2011 Simple Fabrication of Asymmetric High-Aspect-Ratio Polymer Nanopillars by Reusable AAO Templates. *Langmuir* **27** 2132–2137.
- [16] Jeong HE, Lee J-K, Kim HN, Moon SH, Suh KY 2009 A nontransferring dry adhesive with hierarchical polymer nanohairs. *Proc. Natl. Acad. Sci. U.S.A.* **106** 5639-5644.
- [17] Kim T, Jeong HE, Suh KY, Lee HH 2009 Stopped Nanohairs: Geometry-Controllable, Unidirectional, Reversible, and Robust Gecko-like Dry Adhesive. *Adv. Mater.* **21** 2276-2281.
- [18] Lee J-L, Shen Y-K, Lin Y, Chen D-R 2010 The Nano-topology Influence of Osteoblast-like Cell on the Bio-nanostructure Thin Film by Nanoimprint. In Int. Conf. on Nanotechnology and Biosensors, Hong Kong, PR China, December 28-30, 2010.
- [19] Chen G, McCarley RL, Soper SA, Situma C, Bolivar JG 2007 Functional Template-Derived Poly(methyl methacrylate) Nanopillars for Solid-Phase Biological Reactions. *Chem. Mater.* **19** 3855-3857.
- [20] Chen G, McCandless GT, McCarley RL, Soper SA 2007 Integration of large-area polymer nanopillar arrays into microfluidic devices using in situ polymerization cast molding. *Lab Chip* **7** 1424-1427.
- [21] Yoon Y, Lee D-W, Lee J-B 2012 Surface modified nano-patterned SU-8 pillar array optically transparent super-hydrophobic thin film. *J. Micromech. Microeng.* **22** 035012.

- [22] Harriott LR 2001 Limits of Lithography. *P. IEEE* **89** 366-374.
- [23] Reyntjens S, Puers R 2001 A review of focused ion beam applications in microsystem technology. *J. Micromech. Microeng.* **11** 287.
- [24] Skupinski M, Sanz R, Jensen J 2007 Surface patterning by heavy ion lithography using self-assembled colloidal masks. *Nucl. Instrum. Meth. B* **257** 777-781.
- [25] Kustandi TS, Samper VD, Yi DK, Ng WS, Neuzil P, Sun W 2007 Self-Assembled Nanoparticles Based Fabrication of Gecko Foot-Hair-Inspired Polymer Nanofibers. *Adv. Funct. Mater.* **17** 2211-2218.
- [26] Palacio MLB, Bhushan B, Schricker SR 2013 Gecko-inspired fibril nanostructures for reversible adhesion in biomedical applications. *Mater. Lett.* **92** 409-412.
- [27] Fureaux RC, Rigby WR, Davidson AP 1989 The formation of controlled-porosity membranes from anodically oxidized aluminium. *Nature* **337** 147-149.
- [28] Belwalkar A, Grasing E, Van Geertruyden W, Huang Z, Misiolek WZ 2008 Effect of processing parameters on pore structure and thickness of anodic aluminum oxide (AAO) tubular membranes. *J. Membrane Sci.* **319** 192-198.
- [29] Zhao S, Chan K, Yelon A, Veres T 2007 Novel structure of AAO film Fabricated by constant current anodization. *Adv. Mater.* **19** 3004-3007.
- [30] Poinern GEJ, Ali N, Fawcett D 2011 Progress in Nano-engineered anodic aluminum oxide membrane development. *Materials* **4** 487-526.
- [31] Martinson ABF, Elam JW, Hupp JT, Pellin MJ 2007 ZnO Nanotube based Dye-sensitized Solar Cells. *Nano Lett.* **7** 2183-2187.
- [32] Banerjee P, Perez I, Henn-Lecordier L, Lee SB, Rubloff GW 2009 Nanotubular metal-insulator-metal capacitor arrays for energy storage. *Nat. Nanotechnol.* **4** 292-296.
- [33] Lee P-S, Lee O-J, Hwang S-K, Jung S-H, Jee SE, Lee K-H 2005 Vertically Aligned Nanopillar Arrays with Hard Skins Using Anodic Aluminum Oxide for Nano Imprint Lithography *Chem. Mater.* **17** 6181-6185.
- [34] Saedi A, Ghorbani M 2005 Electrodeposition of Ni-Fe-Co alloy nanowire in modified AAO template. *Mater. Chem. Phys.* **91** 417-423.
- [35] Yoo W-C, Lee J-K 2004 Field-dependent Growth patterns of metals electroplated in nanoporous alumina membranes. *Adv. Mater.* **16** 1097-1101.
- [36] Sui YC, Acosta DR, Gonzalez-Leon JA, Bermudez A, Feuchtwanger J, Cui BZ, Flores JO, Saniger JM 2001 Structure, Thermal Stability and deformation of multibranch carbon nanotubes synthesized by CVD in the AAO template. *J. Phys. Chem. B* **105** 1523-1527.
- [37] Guo J, Xu Y, Wang C 2011 Sulfur-Impregnated Disordered Carbon Nanotubes Cathode for Lithium-Sulfur Batteries. *Nano Lett.* **11** 4288-4294.
- [38] Rohrig M, Schneider M, Etienne G, Oulhadj F, Pfannes F, Kolew A, Worgull M, Holscher H 2013 Hot pulling and embossing of hierarchical nano- and micro-structures. *J. Micromech. Microeng* **23** 105014.

- [39] Izadi H, Zhao B, Han Y, McManus N, Penlidis A 2012 Teflon hierarchical nanopillars with dry and wet adhesive properties. *J. Polym. Sci. Pol. Phys.* **50** 846-851.
- [40] Pan CT, Wu TT, Chen MF, Chang YC, Lee CJ, Huang JC 2008 Hot embossing of micro-lens array on bulk metallic glass. *Sensor Actuat. A-Phys.* **141** 422-431.
- [41] Kim DS, Lee HS, Lee J, Kim S, Lee K-H, Moon W, Kwon TH 2007 Replication of high-aspect-ratio nanopillar array for biomimetic gecko foot-hair prototype by UV nano embossing with anodic aluminum oxide mold. *Microsyst. Technol.* **13** 601-606.
- [42] Lee H, Bhushan B 2012 Fabrication and characterization of hierarchical nanostructured smart adhesion surfaces. *J. Colloid Interf. Sci.* **372** 231-238.
- [43] Liu K, Du J, Wu J, Jiang L 2012 Superhydrophobic gecko feet with high adhesive forces towards water and their bio-inspired materials. *Nanoscale* **4** 768-772.
- [44] Chang W-Y, Lin K-H, Wu J-T, Yang S-Y, Lee K-L, Wei P-K 2011 Novel fabrication of an Au nanocone array on polycarbonate for high performance surface-enhanced Raman scattering. *J. Micromech. Microeng.* **21** 035023.
- [45] Plaskolite INC. (USA), OPTIX properties, [cited 2014 Jan 15], Available from: <http://www.plaskolite.com/Fabrication/Acrylic/Optix>.
- [46] Zhang C, Zhou J, Sameoto D, Zhang X, Li Y, Ng HW, Menon C, Gates BD 2014 Determining adhesion of nonuniform arrays of fibrils. *J. Adhes. Sci. Technol.* **28** 320-336.
- [47] SPI supplies/Structure Probe, Inc. (USA), ANOPORE™ Inorganic Aluminum Oxide Membrane Filters, [cited 2014 Jan 15], Available from: http://www.gelifesciences.com/webapp/wcs/stores/servlet/catalog/en/GELifeSciences-ca/products/AlternativeProductStructure_16220/28420418.
- [48] Menon C, Murphy M, Sitti M 2004 Gecko Inspired Surface Climbing Robots. In IEEE Int. Conf. on Robotics and Biomimetics, Shenyang City, PR China, Aug. 22-26, 2004.
- [49] Efimenko K, Wallace WE, Genzer J 2002 Surface Modification of Sylgard-184 Poly(dimethyl siloxane) Networks by Ultraviolet and Ultraviolet/Ozone Treatment. *J. Colloid. Interf. Sci.* **254** 306-315.
- [50] Diversified Enterprises (USA), Critical surface tension and contact angle with water for various polymers, [cited 2014 Jan 15], http://www.accudynetest.com/polytable_03.html?sortby=contact_angle.